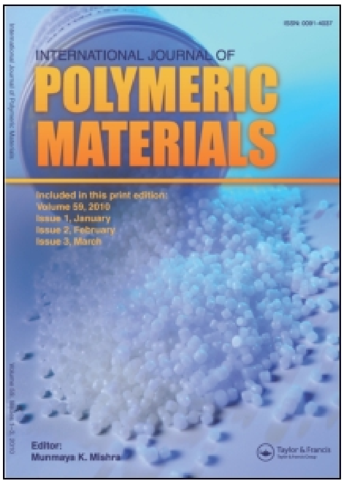

International Journal of Polymeric Materials
Publication details, including instructions for authors and subscription information:
http://www.informaworld.com/smpp/title~content=t713647664

Damping Augmentation of Epoxy Using Carbon Nanotubes

Abdolhosein Fereidoon[a]; Naser Kordani[a]; Morteza Ghorbanzadeh Ahangari[a]; Mohammadreza Ashoory[a]
[a] Department of Mechanical Engineering, Semnan University, Semnan, Iran

To cite this Article Fereidoon, Abdolhosein , Kordani, Naser , Ahangari, Morteza Ghorbanzadeh and Ashoory, Mohammadreza(2011) 'Damping Augmentation of Epoxy Using Carbon Nanotubes', International Journal of Polymeric Materials, 60: 1, 11 — 26

To link to this Article: DOI: 10.1080/00914037.2010.504152

URL: http://dx.doi.org/10.1080/00914037.2010.504152

International Journal of Polymeric Materials, 60:11–26, 2011
Copyright © Taylor & Francis Group, LLC
ISSN: 0091-4037 print/1563-535X online
DOI: 10.1080/00914037.2010.504152

Taylor & Francis
Taylor & Francis Group

Damping Augmentation of Epoxy Using Carbon Nanotubes

Abdolhosein Fereidoon, Naser Kordani, Morteza Ghorbanzadeh Ahangari, and Mohammadreza Ashoory

Department of Mechanical Engineering, Semnan University, Semnan, Iran

In nanotube-based polymeric composite structures it is anticipated that high damping can be achieved by taking advantage of the interfacial friction between the nanotubes and the polymer. The purpose of this paper is to investigate the structural damping characteristics of polymeric composites containing carbon nanotubes (CNT) of various kinds and amounts. The damping characteristics of the specimens with 0, 0.5, 1 and 1.5 wt% nanotube contents were determined experimentally. Through comparing with neat resin specimens, the study showed that one can enhance damping by adding CNT fillers into epoxy. It is also shown that single-walled carbon nanotube (SWCNT)-based composites could achieve higher damping than composites with multi-walled carbon nanotube (MWCNT) fillers. Comparing the damping ratio of 0.5 wt% MWCNT and functionalized MWCNT (MWCNT-COOH) specimens, the damping ratio of the 0.5 wt% MWCNT-COOH specimen is higher because of the surface modification. Similarly, experiments showed that the maximum value of the damping ratio was obtained at 1 wt%.

Keywords carbon nanotube, composite, damping, epoxy, surface modification

INTRODUCTION

Recently, nanoparticles have been attracting increasing attention in the composite community because they are capable of improving the mechanical and physical properties of a polymer matrix [1–6]. Their nanometer size, which leads to high specific surface areas of up to more than 1000 m^2/g, and

---

Received 12 February 2010; accepted 14 April 2010.

Address correspondence to Morteza Ghorbanzadeh Ahangari, Department of Mechanical Engineering, Semnan University, Semnan, Iran. E-mail: ghorbanzadeh.morteza@gmail.com

extraordinary mechanical, electrical and thermal properties, make them unique nano-fillers for structural and multifunctional composites.

Commonly used nanoparticles in nanocomposites include multi-walled carbon nanotubes MWCNTs, single-walled carbon nanotubes SWCNTs, carbon nanofibers (CNFs), montmorillonite (MMT) nanoclays, and polyhedral oligomeric silsesquioxanes (POSS). Other nanoparticles, such as Al_2O_3, TiO_2, and nanosilica are also used in the nanocomposites. Compared to other particulate additives, carbon nanotubes and carbon nanofibers offer a number of advantages. The addition of a small amount of carbon nanotubes or carbon nanofibers can enhance the matrix-dominated properties of composites, such as stiffness, fracture toughness, and interlaminar shear strength [7–11]. The improvement of mechanical properties has been substantiated by a variety of experimental procedures [12–14].

As produced, SWCNTs are found either in parallel bundles referred to as "ropes" or in concentric bundles known as MWCNTs [15,16]. In each bundle arrangement, the SWCNTs are held together with relatively weak van der Waals forces. It has been found that interlayer sliding of MWCNTs is comparable to that of graphene layers in crystalline graphite [16,17].

New fabrication and purification techniques have enhanced the production of carbon nanotubes (CNTs) [18,19], leading to the possibility that lightweight structural polymers with excellent mechanical properties can be produced using small weight/volume fractions of CNTs as a reinforcing phase. For example, with the addition of only 1% nanotubes by weight, a 36–42% increase in elastic modulus has been observed for polystyrene [20]. Experimental results have demonstrated that the improvement of material properties relies on nanotube dispersion and resin/nanotube interfacial bonding [20–24].

Most of the research on CNT-based composites has focused on their elastic properties. Relatively little attention has been given to their damping mechanisms and ability. However, Koratkar et al. [25,26] recently observed promising damping ability for a densely packed MWCNT thin film. They conducted direct shear testing of an epoxy that contained MWCNTs and reported strong viscoelastic behavior with up to 1400% increase in the loss factor of the baseline epoxy resin. The great improvement in damping was achieved without sacrificing the mechanical strength and stiffness of the polymer, and with a minimal weight penalty.

Traditionally, researchers have fabricated CNT composites by directly mixing CNT into polymers and then using casting and injection techniques to make nanocomposites. However, it should be noted that melt mixing is the most preferred method for the preparation of polymer/CNT nanocomposites for industrials applications [27]. Gou et al. [28] developed a new technique approach to fabricate nanocomposites using SWCNT. The experimental details of their fabrication of SWCNT were described in a different paper [29,30].

Previous research has explored the effects of nanoscale particle fillers on the damping properties of polymer composites. For elastomeric materials, it has been found that rod-like aggregates of roughly spherical carbon black particles increased the material damping in the strain range in which the breakdown and reformation of carbon black aggregates occurs [31,32]. This strain dependent, damping enhancement in particle-filled elastomers is known as the Payne Effect. Analogous effects can be expected for composites containing CNT fillers.

Because of the small size of nanotubes, the surface area to mass ratio (specific area) of carbon nanotube arrays is extremely large. Therefore, in composites with CNT fillers, it is anticipated that high damping can be achieved by taking advantage of the weak bonding and interfacial friction between individual CNTs and resin. Recently, Buldum and Lu [33] investigated the interfacial sliding and rolling of carbon nanotubes using MD methods. It was found that a nanotube first sticks and then slips suddenly when the force exerted on it is sufficiently large. The resulting hysteresis observable in the plot of force versus distance provided the energy dissipated during the "stick-slip" motion.

The main goal of this paper was to explore the damping properties of epoxy and its nanocomposites reinforced with different amounts and various kinds of CNT.

THEORY

The damping of a structure can be estimated using the well known half-power point method [34]. This theory calculates the frequency response function (FRF) of a structure. The sharpness of resonance related to one of the modes of the vibrating structure can be used to estimate the damping ratio of that mode. Figure 1 shows the half-power points related to one resonance peak of the structure.

Damping can be calculated from Eq. (1)

$$\xi = \frac{\omega_2^2 - \omega_1^2}{4\omega_n^2} \approx \frac{\omega_2 - \omega_1}{2\omega_n} \tag{1}$$

where ω(Hz) is the excitation frequency, ω_1(Hz), ω_2(Hz) are the frequencies corresponding to the half-power point, and ω_n(Hz) is the natural frequency.

The half-power point method is mainly applicable for lightly damped structures. Figure 2 indicates a heavily damped resonance peak of a vibrating system. For heavily damped structures, Eq. (1) can be modified as follows:

Around a mode, the dynamic behavior of system can be considered as a single degree of freedom system (SDOF) [34]. Figure 3 indicates a model of a SDOF system. For a SDOF system we have:

$$X = \frac{\frac{F_0}{K}}{\sqrt{(1 - (\frac{\omega}{\omega_n})^2)^2 + (2\xi\frac{\omega}{\omega_n})^2}} \tag{2}$$

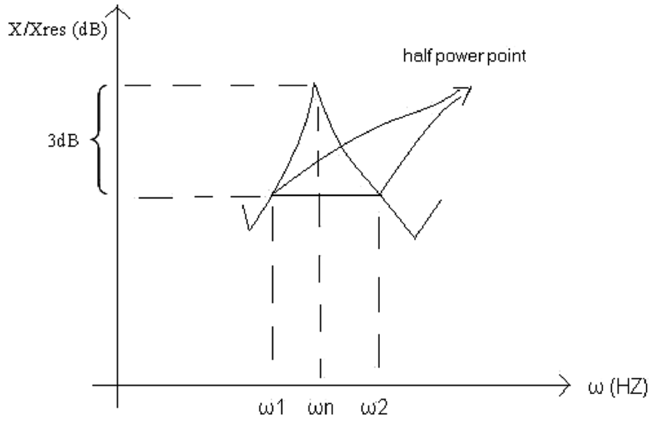

Figure 1: The half-power point's technique related to one resonance peak of the structure.

where m and K are the mass and stiffness of the spring, ξ is the damping ratio, X is amplitude of vibration, X_{RES} is amplitude at resonance and F_0 is the excitation amplitude.

For a heavily damped structure the level of $X_{RES} - 1.5\,\text{db}$ can be considered instead of $X_{RES} - 3\,\text{db}$ in the half-power point method; thus we have:

$$20 \log \frac{X}{X_{RES}} = -1.5 \text{ db} \tag{3}$$

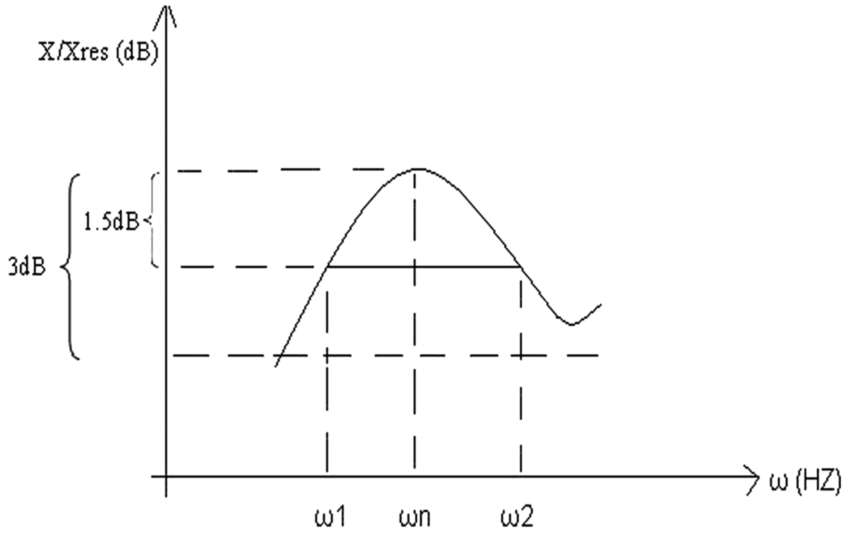

Figure 2: Indicates a heavily damped resonance peak of a vibrating system.

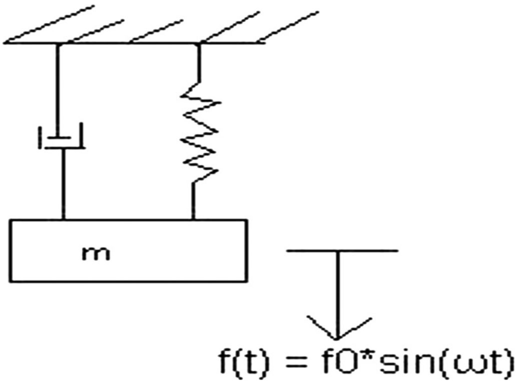

Figure 3: A single degree of freedom system (SDOF).

$$\frac{X}{X_{RES}} = 0.84 \tag{4}$$

$$X_{RES} = \frac{F_0 / K}{2\xi} \tag{5}$$

Substituting Eqs. (4) and (5) into Eq. (2), for $\xi \ll 1$, we have:

$$(\omega/\omega_n)^2 = 1 \pm 1.3\xi \tag{6}$$

For $\omega < \omega_n$, $\omega = \omega_1$ and for $\omega > \omega_n$, $\omega = \omega_2$.

$$\omega_1^2 = (1 - 1.3\xi)\omega_n^2 \tag{7}$$

$$\omega_2^2 = (1 + 1.3\xi)\omega_n^2 \tag{8}$$

With subtraction we have:

$$2.6\ \xi = \frac{\omega_2^2 - \omega_1^2}{\omega_n} \tag{9}$$

EXPERIMENT

Specimen Preparation

An epoxy resin (LY 564 from Huntsman) with a polyamide hardener (HY 560 from Huntsman) was employed as a matrix in this study, with unidirectional carbon fiber (T300) as filler. In order to evaluate the CNT effect on a fiber-reinforced polymer composite, different types of CNTs were also dispersed in the matrix. Chemical vapor deposition (CVD)-technique-produced CNT, from the Research Institute of Petroleum Industry (RIPI) were used. The MWCNT had an outer diameter of 23 nm and an inner diameter of 11 nm and the SWCNTs diameters were between 1 and 4 nm and the maximum length was less than 10 μm; moreover, these CNT were functionalized by oxidation and ultraviolet ray techniques from RIPI. Figure 4 shows carbon nanotube TEM images before and after functionalization; the dark points are metal particles and amorphous carbon materials. With acid treatment, the metal catalyst was eliminated, the closed tubes were opened and the length of nanotubes was shortened [35–37]. In agreement with TEM investigation, EDX analysis of the acid-treated samples showed a decrease in the metal catalyst (cobalt).

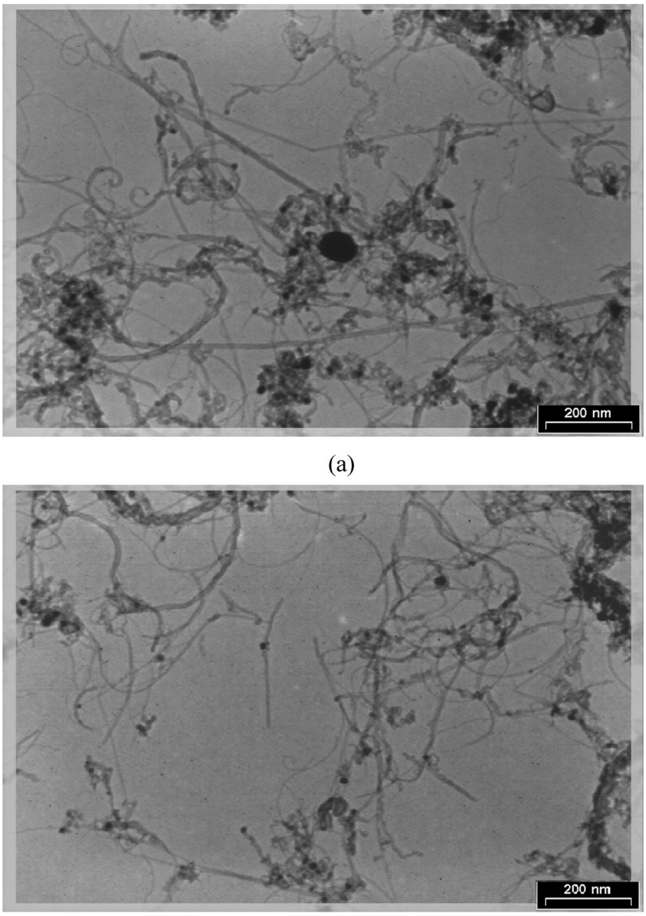

(a)

(b)

Figure 4: (a) Carbon nanotube micrograph before functionalization, (b) carbon nanotube micrograph after functionalization.

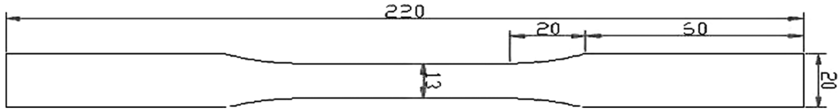

Figure 5: Specimens prepared by cutting a nanocomposite plate (units are in millimeter).

For simplicity, the same weight fraction each of SWCNT, MWCNT or functionalized MWCNT (MWCNT_COOH) (0.5 wt%) was dispersed directly into the hardener (HY560) with ultrasonic for 10 min with 60% power. After sonication, a high shear mixer was used at 700 rpm for 30 min to achieve better dispersion in the hardener. The epoxy resin (LY 564) was degassed first and then mixed with the HY560/CNT mixture. A composite plate was left for 15 h at 50°C under a vacuum bag after it was prepared with hand lay-up. Specimens were prepared by cutting the composite plate into small pieces with a saw (220 mm × 13–20 mm × 5 mm), as shown in Figure 5.

The processes were the same for MWCNT-COOH, SWCNT, and MWCNT. The formulations of the nanocomposites are presented in Table 1.

Scanning electron microscopy (SEM) was performed using a Cambridge S360 to examine the fracture surface morphology of the epoxy/CNT nanocomposites. The fracture surface was prepared by fracturing the epoxy/CNT nanocomposites in liquid nitrogen. The sample was sputtered with gold prior to observation. SEM photos were taken to evaluate the nanotube dispersion in the resin, as shown in Figure 6, which is for a 0.5 wt% MWCNT.

Modal Testing and Analysis

A regular composite beam without nanotube and nanocomposite beams with carbon nanotubes were used as the specimens for the damping test.

A force transducer (BK8200) was attached on one side of the specimen to measure the input force. An accelerometer (A/123E) was attached on the other side of the specimen to detect the acceleration, as shown in Figure 7. The specimen was in a free-free boundary condition and was excited by a shaker (BK4808).

Sweep sinusoidal signals were used as the excitation source for shaker, and the frequency response function (FRFs) was derived using an Analyzer in a conventional modal testing procedure.

Figures 8–13 show the measured FRFs for specimens with different nanotube material contents (0, 0.5, 1 and 1.5 wt%). The damping ratios for these specimens were computed according to the theoretical procedure.

Table 1: Damping ratio calculated by modified half-power method

	1st mode Frequency (Hz)	1st mode damping ratio	2st mode Frequency (Hz)	2st mode damping ratio	3st mode Frequency (Hz)	3st mode damping ratio
Regular composite beam	118	0.036	272	0.028	580	0.023
Nanocomposite beam Epoxy/SW/0.5 wt%	129	0.081	318	0.21	682	0.102
Nanocomposite beam Epoxy/MW/0.5 wt%	122	0.071	306	0.153	652	0.84
Nanocomposite beam Epoxy/MW-COOH/ 0.5 wt%	123	0.085	309	0.322	680	0.122
Nanocomposite beam Epoxy/MW-COOH/ 1 wt%	117	0.096	295	0.336	623	0.121
Nanocomposite beam Epoxy/MW-COOH/ 1.5 wt%	124	0.070	320	0.171	685	0.125

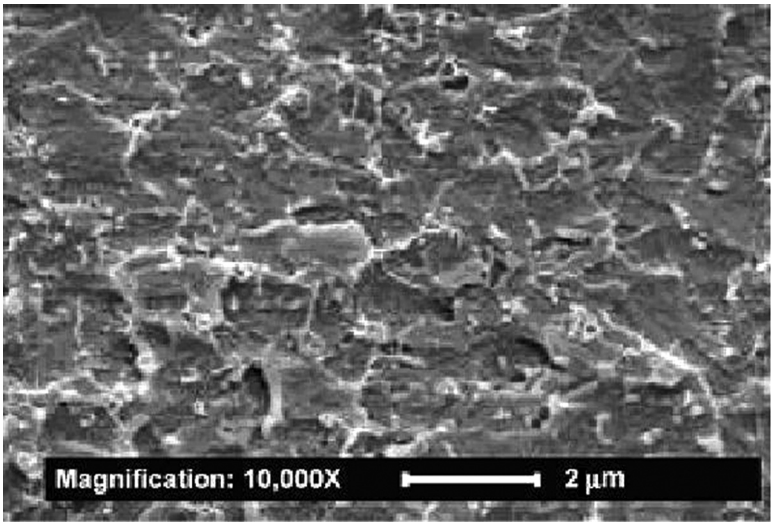

Figure 6: SEM microphoto of epoxy/MWCNT nanocomposite with 0.5 wt% MWCNT material.

Figure 7: Experimental setup for the damping test.

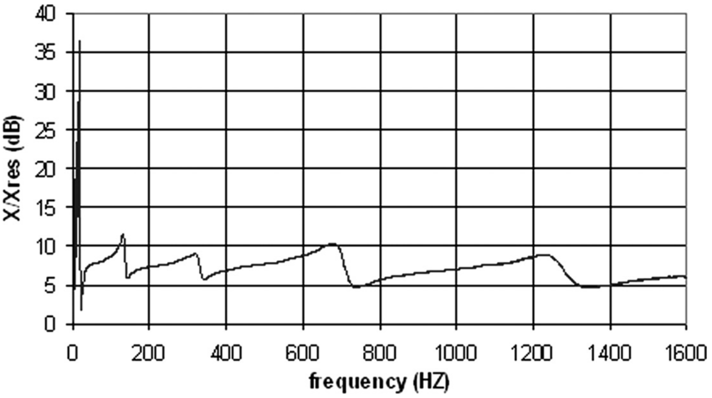

Figure 8: Frequency response function for 0.5 wt% SWCNT nanocomposite.

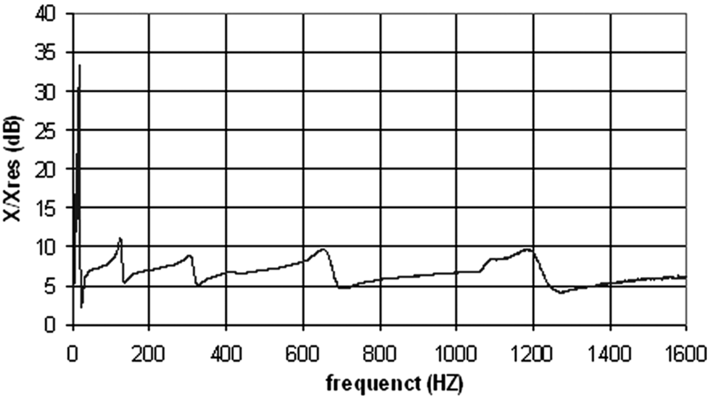

Figure 9: Frequency response function for 0.5 wt% MWCNT nanocomposite.

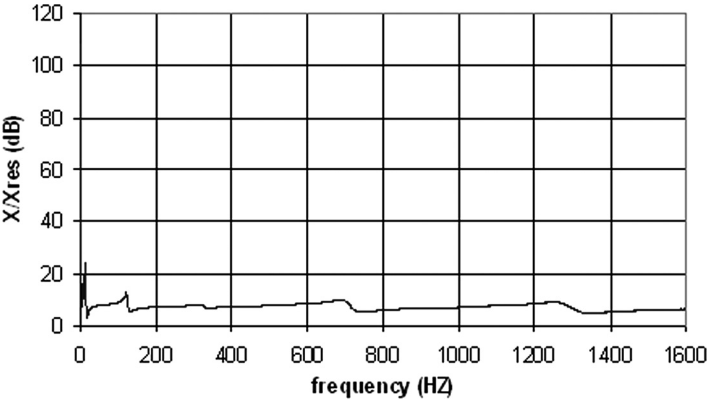

Figure 10: Frequency response function for 0.5 wt% MWCNT-COOH nanocomposite.

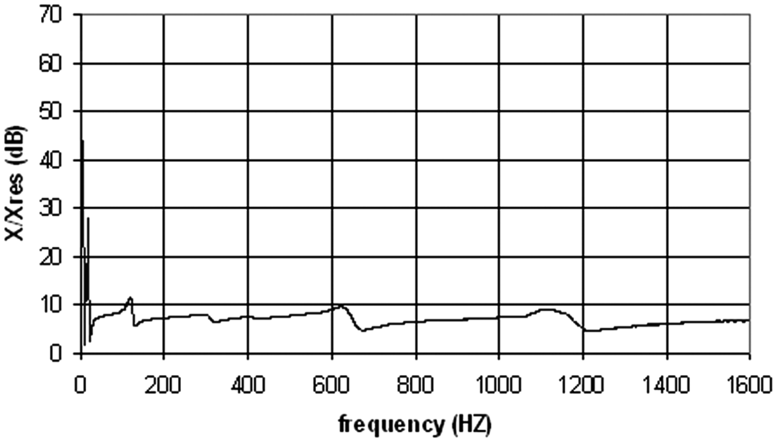

Figure 11: Frequency response function for 1 wt% MWCNT-COOH nanocomposite.

RESULTS AND DISCUSSION

Experimental investigations were performed to obtain the damping ratio of the neat specimens, and the damping characteristics of the CNT-based composites.

The damping characteristics of the specimens with 0.5, 1 and 1.5 wt% nanotube content were shown in Figures 8–12. Comparing Figure 13 with Figures 8–12, it can be seen that the damping characteristics of the beams were significantly different between specimens with and without nanotubes. It is also apparent that damping can be enhanced by adding CNTs.

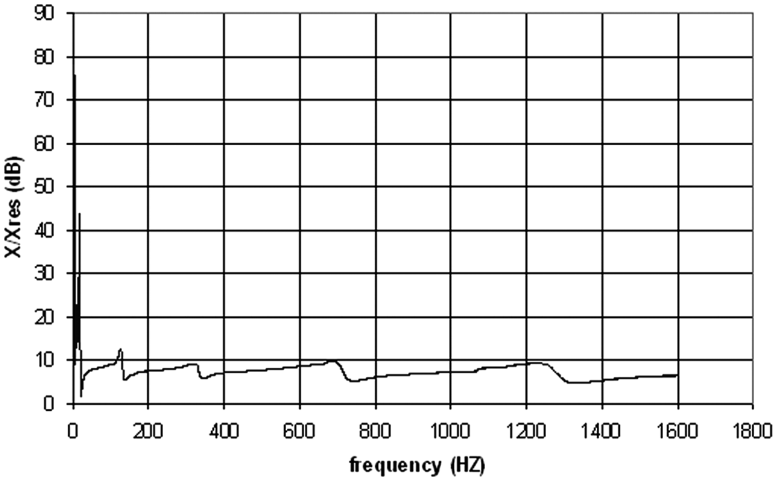

Figure 12: Frequency response function for 1.5 wt% MWCNT-COOH nanocomposite.

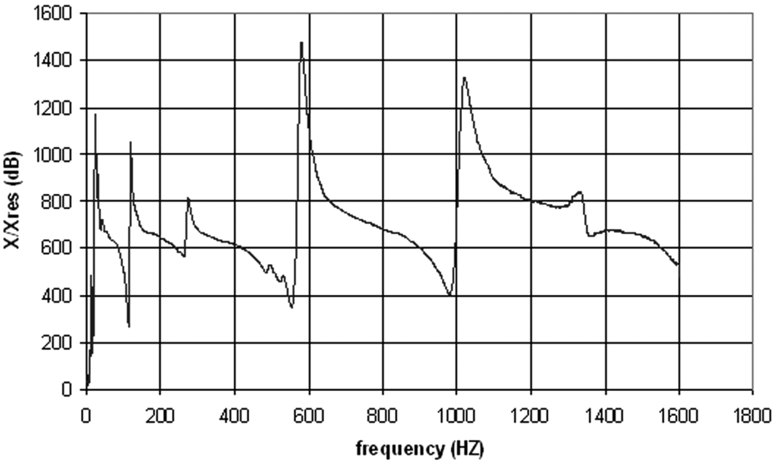

Figure 13: Frequency response function for epoxy.

The damping ratio of the 1 wt% specimen is much higher than those of the 0.5 and 1.5 wt% specimens and the neat specimen.

Comparing the damping ratios of the 0.5 wt% MWCNT, SWCNT, MWCNT-COOH specimens it can be seen that the damping ratio of the 0.5 wt% SWCNT-specimen is greater than that of the 0.5 wt% MWCNT because of the van der Waals force between the nanotube layers. Figure 14 shows that the damping ratio of the 0.5 wt% MWCNT-COOH_specimen is greater than that of the 0.5 wt% MWCNT because of surface modification. The damping ratio of the regular composite beam and the nanocomposite beam are compared in Figure 15.

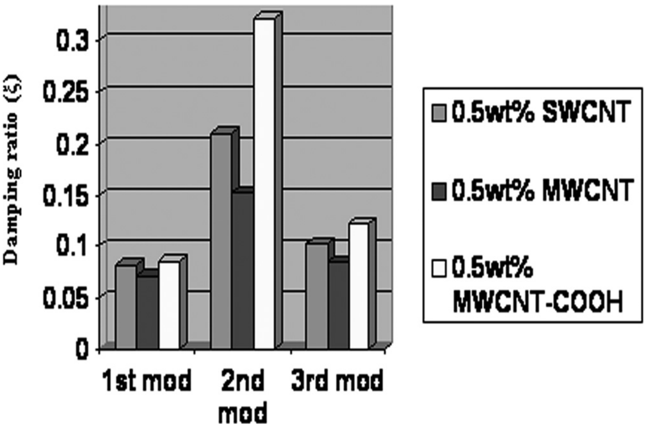

Figure 14: Damping ratio of the 0.5 wt% MWCNT, SWCNT, MWCNT-COOH specimens are compared for the first, second, and third natural frequencies.

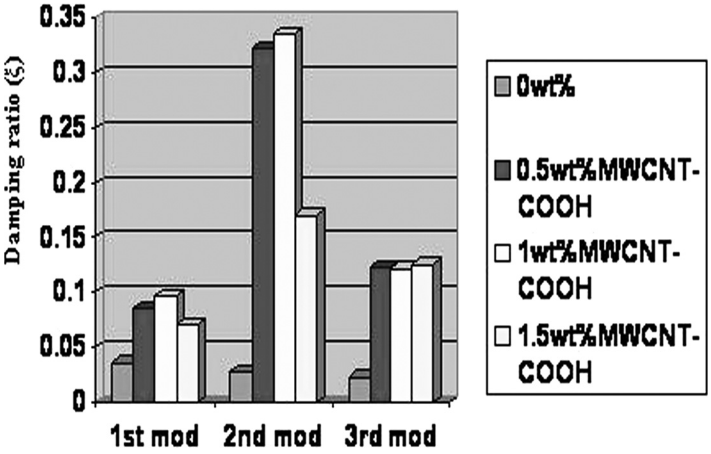

Figure 15: Damping ratio of the regular composite beam and the nanocomposite beams for the first, second, and third natural frequencies.

The peak value in the FRF represents resonance at a certain frequency. From the FRF, it can be clearly seen that the sharp peak of the first mode, second mode, and third mode are significantly reduced for the nanocomposite beam, which indicates that the nanocomposite beam has improved the damping property.

To further demonstrate the improved damping of the nanocomposite beam, the frequency responses of the regular Composite beam and the nanocomposite beam are compared in Table 1.

This comparison demonstrates that the damping ratio values of the nanocomposite beam at these three natural frequencies are much greater than those of the regular composite beam. The damping ratio is calculated by using Eq. (9).

Table 1 show the first three modal frequencies and associated damping ratios of the six beams. From the damping ratio comparison, it is clear that the damping ratio of the nanocomposite beam increased up to 200–1200% at the 2nd mode and 3rd mode frequencies. However, there is little change in the mode frequencies, which means that there is only a slight change in the stiffness of the composites. This demonstrates an advantage of nanocomposite over regular composite.

Therefore, it is concluded that the incorporation of carbon nanotubes could result in a significant increase in structural damping of conventional fiber-reinforced composites.

CONCLUSION

Given that more energy will be dissipated with a greater frictional force, the interfacial area between the nanotubes and the resin is extremely large because of the small size of carbon nanotubes, which will cause greater frictional force and structural damping.

It can be observed that the composites with MWCNTs have much higher damping ratios than that of the neat resin specimen. This higher damping ratio is due to the fact that nanotube-based composites have the largest interfacial contact area with the resin, and the highest stiffness among all the different fillers considered.

Note that with greater stiffness, fillers have an increased capability to resist applied loading, which could lead to more slippage and energy dissipation through friction. In other words, the increase in contact area dramatically increases the potential for energy dissipation due to interfacial friction.

Nevertheless, it can be concluded that, by taking advantage of the large interfacial contact area between CNTs and resins, as well as the high stiffness and low density properties of CNTs, high performance in energy dissipation and structural damping can be achieved by the proposed treatment.

It can be observed that with increased MWCNT-COOH weight ratio up to 1 wt%, the damping ratio increases. This is due to the fact that more energy will be dissipated with a larger frictional force.

The damping ratio decreases for a weight ratio of 1.5 wt%; these decreases are due to inherent van der Waals attractions between nanotubes that readily cause the formation of more entangled agglomerates in the epoxy matrix. This gives rise to defects in the epoxy and decreases adhesion nanofiller to the matrix. However, the elongation at a break decreases considerably, even for 0.5 wt% MWNTs.

This reduction may be due to the poor interfacial interaction of the MWNTs with the epoxy matrix because of the nanopolarity of the MWNTs and the epoxy. Defects introduced into the polymer matrix from the addition of MWNTs also contributed to this reduction.

Because of the higher aspect ratio and high surface area of the nanotubes, it seems to be impossible to disperse the MWCNT properly when the greater amounts of filler are incorporated into a matrix, especially by the melt-mixing method.

Similarly experiments showed that the maximum damping ratio was obtained at 1 wt%.

From Figure 14, it can be observed that the composites with MWCNT-COOH have a much higher damping ratio than the composites with MWCNTs.

REFERENCES

[1] Breuer, O. and Sundararaj, U. *Polym. Compos.* **25**, 630 (2004).

[2] Thostenson, E. T., Ren, Z., and Chou, T. W. *Compos. Sci. Technol.* **61**, 1899 (2001).

[3] Lau, K. T., and Hui, D. *Compos. B. Eng.* **33**, 263 (2002).

[4] Gojny, F. H., Wichmann, M. H. G., Fiedler, B., Bauhofer, W., and Schulte, K. *Compos. A. Appl. Sci. Manufact.* **36**, 1525 (2005).

[5] Anand, A., Jose, S., Alex, R., and Joseph, R. *Int. J. Polym. Mater.* **59**, 33 (2010).

[6] Chozhan, C. K., Rajasekaran, R., Alagar, M., and Gnanasundaram, P. *Int. J. Polym. Mater.* **57**, 319 (2008).

[7] Gojny, F. H., Wichmann, M. H. G., Köpke, U., Fiedler, B., and Schulte, K. *Compos. Sci. Technol.* **64**, 2363 (2004).

[8] Qian, D., Dickey, E. C., Andrews, R., and Rantell, T. *Appl. Phys. Lett.* **76**, 2868 (2000).

[9] Schadler, L. S., Giannaris, S. C., and Ajayan, P. M. *Appl. Phys. Lett.* **73**, 3842 (1998).

[10] Ma, H., Zeng, J., Realff, M. L., Kumar, S., and Schiraldi, D. A. *Compos. Sci. Technol.* **63**, 1617 (2003).

[11] Bower, C., Rosen, R., Jin, L., Han, J., and Zhou, O. *Appl. Phys. Lett.* **74**, 3317 (1999).

[12] Salvetat, J. P., Bonard, J. M., Thomson, N. H., Kulik, A. J., Forró, L., and Benoit, W. *Appl. Phys. A.* **69**, 255 (1999).

[13] Treacy, M. M. J., Ebbesen, T. W., and Gibson, J. M. *Nature* **381**, 678 (1996).

[14] Wong, E. W., Sheehan, P. E., and Lieber, C. M. *Science* **277**, 1971 (1997).

[15] Wagner, H. D., Lourie, O., Feldman, Y., and Tenne, R. *Appl. Phys. Lett.* **72**, 188 (1998).

[16] Yu, M. F., Lourie, O., Moloni, K., Dyer, M. J., Kelly, T. F., and Ruoff, R. S. *Science* **287**, 637 (2000).

[17] Ru, C. Q. *J. Appl. Phys.* **87**, 7227 (2000).

[18] Chiang, I. W., Brinson, B. E., Smalley, R. E., Margrave, J. L., and Hauge, R. H. *J. Phys. Chem. B.* **105**, 1157 (2001).

[19] Colomer, J. F., Stephan, C., Lefant, S., Van Tendeloo, G., Willem, I., Kónya, Z., et al. *Chem. Phys. Lett.* **317**, 83 (2000).

[20] Qian, D., Dickey, C., Andrews, R., and Rantell, T. *Appl. Phys. Lett.* **76**, 2868 (2000).

[21] Ajayan, P. M., Schadler, L. S., Giannaris, C., and Rubio, A. *Adv. Mater.* **12**, 750 (2000).

[22] Sandler, J., Shaffer, M. S. P., Prasse, T., Bauhofer, W., Schulte, K., and Windle, A. H. *Polymer* **40**, 5967 (1999).

[23] Schadler, L. S., Giannaris, S. C., and Ajayan, P. M. *Appl. Phys. Lett.* **73**, 3842 (1998).

[24] Thostenson, E. T., Ren, Z. F., and Chou, T. W. *Compos. Sci. Technol.* **61**, 1899 (2001).

[25] Koratkar, N. A., Wei, B., and Ajayan, P. M. *Compos. Sci. Technol.* **63**, 1525 (2003).

[26] Koratkar, N. A., Wei, B., and Ajayan, P. M. *Adv. Mater.* **14**, 997 (2002).

[27] Bhattacharyya, A. R., Pötschke, P., Häußler, L., and Fischer, D. *Macromol. Chem. Phys.* **206**, 2084 (2005).

[28] Gou, J., Minaie, B., Wang, B., Liang, Z., and Zhang, C. *Comput. Mater. Sci.* **31**, 225 (2004).

[29] Wang, Z., Liang, Z., Wang, B., Zhang, C., and Kramer, L. *Compos. A. Appl. Sci. Manufact.* **35**, 1225 (2004).

[30] Gou, J., Liang, Z., and Wang, B. *Int. J. Nanoscience.* **3**, 293 (2004).

[31] Payne, A. R., and Whittaker, R. E. *Rubber. Chem. Tech.* **44**, 440 (1971).

[32] Slösberg, M., and Kari, L. *Polym. Test.* **22**, 343 (2003).

[33] Buldum, A., and Lu, J. P. *Phys. Rev. Lett.* **83**, 5050 (1999).

[34] Thomson, W. T., and Teylor, W. *Theory of Vibration with Applications*, (George Allen & Unwin, London).

[35] Zhang, Y., Shi, Z., Gu, Z., and Iijima, S. *Carbon* **38**, 2055 (2000).

[36] Jung, D. H., Koan, K. O. Y., and Jung, H. T. *Mater. Sci. Eng. C.* **24**, 117 (2004).

[37] Marshal, M. W., Popa-Nita, S., and Shapter, J. G. *Carbon* **44**, 1137 (2006).